In Vivo Detection of Succinate by Magnetic Resonance Spectroscopy as a Hallmark of SDHx Mutations in Paraganglioma

Charlotte Lussey-Lepoutre, Alexandre Bellucci, Aur Elie Morin, Alexandre Buffet, Laurence Amar, Maxime Janin, Chris Ottolenghi, Franck E Zinzindohou, Gwennhael Autret, Nelly Burnichon, et al.

Biology of Human Tumors

Clinical Cancer Research

In vivo detection of succinate by magnetic resonance spectroscopy as a hallmark of *SDH*x mutations in paraganglioma

Charlotte Lussey-Lepoutre†[1,2], Alexandre Bellucci†[1,2], Aurélie Morin[1,2], Alexandre Buffet[1,2], Laurence Amar[1,2,3], Maxime Janin[2,4,5], Chris Ottolenghi[2,4,5], Franck Zinzindohoué[2,6], Gwennhael Autret[1,2], Nelly Burnichon[1,2,7], Estelle Robidel[1,2], Benjamin Banting[8], Sébastien Fontaine[8], Charles-André Cuenod[1,2,8], Paule Benit[9,10], Pierre Rustin[9,10], Philippe Halimi[2,8], Laure Fournier[1,2,8], Anne-Paule Gimenez-Roqueplo[1,2,7], Judith Favier[#*1,2] and Bertrand Tavitian[#1,2,8]

[1]INSERM, UMR970, Paris Cardiovascular Research Center, Paris, France.
[2]Université Paris Descartes, Sorbonne Paris Cité, Faculté de Médecine, Paris, France.
[3]Assistance Publique-Hôpitaux de Paris, Hôpital Européen Georges Pompidou, Service d'hypertension artérielle et médecine vasculaire, F-75015 Paris, France.
[4]Assistance Publique-Hôpitaux de Paris, Hôpital Necker-Enfants Malades, Laboratoire de Biochimie Métabolique, Paris, France.
[5]INSERM, U1124, Paris, France.
[6]Assistance Publique-Hôpitaux de Paris, Hôpital Européen Georges Pompidou, Service de Chirurgie Digestive, F-75015 Paris, France.
[7]Assistance Publique-Hôpitaux de Paris, Hôpital Européen Georges Pompidou, Service de Génétique, Paris, France
[8]Assistance Publique-Hôpitaux de Paris, Hôpital Européen Georges Pompidou, Service de Radiologie, Paris, France.
[9]INSERM, UMR1141, Hôpital Robert Debré, Paris, France.
[10]Université Paris 7, Faculté de Médecine Denis Diderot, Paris, France.

† C. Lepoutre-Lussey and A. Bellucci contributed equally to this work.
# J. Favier and B. Tavitian jointly directed this work.

Running title: *In vivo* detection of succinate in paraganglioma

Key words: Succinate, magnetic resonance spectroscopy, imaging, paraganglioma, pheochromocytoma

Funding: This work received funding from the Cancer Research for Personalized Medicine - CARPEM project (Site de Recherche Intégré sur le Cancer - SIRIC), the Agence Nationale de la Recherche (ANR-2011-JCJC-00701 MODEOMAPP), the European Union Seventh Framework Programme (FP7/2007-2013) under grant agreement n° 259735, the Institut National du Cancer et la Direction Générale de l'Offre de Soins (INCa-DGOS_8663) for the COMETE network.

Conflict of interests: We have no conflict interests to disclose

***Corresponding author:** Dr. Judith Favier
PARCC- Centre de recherche cardiovasculaire de l'HEGP
56 rue Leblanc 75015 Paris, France
E-mail: judith.favier@inserm.fr
Tel: 01 53 98 80 41 - Fax: 01 53 98 79

Word count (excluding references):4155

Total number of figures and tables: 5

Statement of translational relevance

A large proportion of patients with paraganglioma/pheochromocytoma (PPGL) carry a germline mutation in an SDHx gene. Identification of *SDHx* mutations is important for the diagnostic work-up, the management, and the follow-up of patients with PPGL and their families, which are at risk of developing multiple PGL. Moreover, *SDHB* gene mutations predispose to malignant, particularly aggressive forms of the disease. Therefore, a genetic counseling is now recommended for all patients suffering from PPGL. We here show that in vivo detection of succinate by proton magnetic resonance spectroscopy is a highly specific and sensitive hallmark of *SDHx* mutated tumors. This noninvasive approach will allow identifying and classifying SDHx mutations or variants of unknown significance. It may help for the characterization of inoperable tumors and suspicious lesions, and serve as a surrogate biomarker in the assessment of tumor response to specific treatments.

Abstract

Purpose

Germline mutations in genes encoding mitochondrial succinate dehydrogenase (SDH) are found in patients with paragangliomas, pheochromocytomas, gastrointestinal stromal tumors, and renal cancers. SDH inactivation leads to a massive accumulation of succinate, acting as an oncometabolite and which levels, assessed on surgically resected tissue are a highly specific biomarker of SDHx-mutated tumors. The aim of this study was to address the feasibility of detecting succinate in vivo by magnetic resonance spectroscopy.

Experimental design

A pulse proton magnetic resonance spectroscopy (^{1}H-MRS) sequence was developed, optimized and applied to image nude mice grafted with *Sdhb*$^{-/-}$ or wild-type chromaffin cells. The method was then applied to paraganglioma patients carrying (n=5) or not (n=4) an *SDHx* gene mutation. Following surgery, succinate was measured using gas chromatography-mass spectrometry and SDH protein expression was assessed by immunohistochemistry in resected tumors.

Results

A succinate peak was observed at 2.44 ppm by ^{1}H-MRS in all *Sdhb*$^{-/-}$-derived tumors in mice and in all paragangliomas of patients carrying an *SDHx* gene mutation, but neither in wild-type mouse tumors nor in patients exempt of *SDHx* mutation. In one patient, ^{1}H-MRS results led to the identification of an unsuspected *SDHA* gene mutation. In another case, it helped defining the pathogenicity of a variant of unknown significance in the *SDHB* gene.

Conclusions

Detection of succinate by ^{1}H-MRS is a highly specific and sensitive hallmark of *SDHx* mutations. This noninvasive approach is a simple and robust method allowing *in vivo* detection of the major biomarker of *SDH*-mutated tumors.

Introduction

Pheochromocytoma (PCC) and paraganglioma (PGL) are rare neuroendocrine tumors that arise in chromaffin cells of the adrenal medulla and in sympathetic and parasympathetic ganglia, respectively. The prevalence of pheochromocytoma and paraganglioma (PPGL) in patients with hypertension consulting at general outpatient clinics is estimated at 0.2 - 0.6 %, but this number may be underestimated (1). Nearly 40 % of patients with PPGL carry a germline mutation in one of the 13 PPGL predisposing genes identified so far (2) and mutations of *SDHx* genes (*SDHA, SDHB, SDHC, SDHD, SDHAF2*) are causative of approximately half of the genetically determined cases. *SDHx* mutations predispose to the hereditary PPGL syndrome but may also be found in patients with gastrointestinal stromal tumors (GIST) (3) or renal clear cell carcinomas (4).

SDHA, B, C, and *D* genes encode the four subunits of succinate dehydrogenase (SDH), a mitochondrial enzyme of the tricarboxylic acid (TCA) cycle that oxidizes succinate into fumarate. They were the first genes encoding a mitochondrial enzyme demonstrated to act as tumor suppressor genes (5), an important finding supporting the hypothesis of a direct link between mitochondrial dysfunction and cancer proposed by Otto Warburg in 1924 (6). Since then, mutations in genes encoding for the TCA enzymes fumarate hydratase (*FH*) (7), isocitrate dehydrogenase (*IDH1* and *2*) (8) and more recently malate dehydrogenase (*MDH2*), were reported to predispose to PPGL, renal cancers, leimyomas, or to be causative of sporadic gliomas (for review, (9)).

Identification of *SDHx* mutations is important for the diagnostic work-up, the management, and the follow-up of index cases and their families. *SDHx*-mutation carriers are at risk of developing

multiple PGL that can arise all along the embryonic migration way of neural crest cells, from the base of the skull to the pelvis (10). Moreover, the identification of *SDHB* gene mutations is of specific clinical importance as they predispose to malignant, particularly aggressive forms of the disease (11, 12), and a genetic counseling is now recommended for all patients suffering from PPGL (1). In familial PPGL patients carrying a germline heterozygous mutation on an *SDHx* gene, the somatic loss of the remaining allele induces a complete SDH loss-of-function, which results in the accumulation of succinate. Succinate acts as an oncometabolite and is suspected to mediate most, if not all of the tumorigenic effects related to *SDHx* mutations (9, 13, 14). Development of specific tumor biomarkers allowing the rapid identification of these patients would be highly beneficial, and particularly helpful for the characterization of inoperable tumors and suspicious lesions. Biomarkers could serve as surrogate markers in the assessment of tumor response to specific treatments. Until now, no *in vivo* method to assess the functional consequences of *SDHx* mutations was available, and all existing tests were performed on surgical resected specimens (15-22).

Succinate concentrations in the millimolar range - 4 to 500 micromoles per gram depending on studies and procedures - have been reported in *SDHx*-mutated PPGL tumors, an increase of up to 100-fold compared to non-*SDHx*-mutated PPGL tumors (19, 21, 23). We hypothesized that these succinate levels could be detected noninvasively by *in vivo* proton magnetic resonance spectroscopy (^{1}H-MRS) in *SDHx*-mutated tumors, without the need for tissue sampling, similarly to 2-hydroxyglutarate in patients with *IDH1/2*-mutated gliomas (24-26). Here, we report a new method for SUCCinate Estimation by Spectroscopy (SUCCES) in patients with PPGL related or not to an *SDHx* mutation.

Materials and Methods

Optimization of SUCCES for succinate detection with ^{1}H-MRS

We first tested the SUCCES sequence at 4.7 Tesla on a 3cm-diameter spherical phantom tube containing 100 mM sodium succinate dibasic hexahydrate, 100 mM L-lactate and animal fat. Spectra and signal intensities acquired with different echo times (TE) ranging from 12.8 to 792 ms are shown in Fig. S1A and S1B. The gradual decrease of the lipid signal with increasing TE eventually unmasked the succinate peak at TE > 70 ms and the lactate peak at TE > 100 ms. As previously described (27), increasing TE reduced the succinate signal exponentially and the lactate peak sinusoidally due to scalar coupling effect (Fig. S1B). In order to study both the succinate and lactate signals, we chose a TE of 272 ms that reduced fat contamination and yielded positive lactate and succinate peaks. We then performed ^{1}H-MRS spectra with decreasing [10-1 mM] concentrations of succinate and lactate (TR: 3000 ms, TE: 272 ms, Average: 128, VOI size 5×5×5 mm). Water suppression was performed using VAPOR pulses (sinc RF pulses, 646 ms total duration, 700 Hz bandwidth), followed by crusher gradients (3 ms duration, 58 mT/m strength). 3-sinc-shaped RF pulses with 4 kHz bandwidth to obtain a spectral width of 20 ppm achieved VOI selection. Spectral resolution was 0.98 Hz/point. After zero filling and phase correction, data filtration was performed with a Gaussian function at the top of the Free Induction Decay, with a length band of 2 Hz and visualization was obtained with a Fourier transform. The area under the succinate peak measured from the spectra was linearly correlated with the succinate concentration (Fig. S1C and S1D).

A similar procedure was performed in the 3T clinical scanner using 3 cm-diameter phantom tubes and a larger VOI size (10 x 10 x 10 mm), except that the TE was lowered to 144 ms to compensate the lower detection threshold and the decrease of the signal-to-noise ratio (Fig. S1E). Based on these procedures, the threshold for succinate detection was found to be approximately 1mM in both magnets.

Generation of the allografted mouse model

No animal model of SDH-related PPGL being available, we generated an allografted mouse model by subcutaneous injection of 2.5×10^6 immortalized mouse chromaffin cells (imCC) (13) carrying a homozygous knockout of the *Sdhb* gene (*Sdhb*$^{-/-}$, clone 8) or their wild type (WT) counterparts *(Sdhb*$^{lox/lox}$*)* into the flanks of 10-weeks old female NMRI-nu mice. Animal experiments were registered by the French Ethical committee under Number 14-041 and followed the ARRIVE guidelines of the National Centre for the Replacement, Refinement, and Reduction of Animals in Research (London, UK).

Tumors were allowed to grow until their size reached 0,6 cm^3. They were then resected and 8 mm^3 fragments were grafted in the dorsal fat pad of naive nude mice. The tumors grew in 100% of mice and tumors were macroscopically visible after 2 weeks for WT and 1 month for *Sdhb*$^{-/-}$ tumors, in line with the reduced growth rate of *Sdhb*$^{-/-}$ cells observed *in vitro* (13). Immediately after magnetic resonance spectroscopy, tumors were retrieved and snap frozen in liquid nitrogen or fixed in 4% paraformaldehyde.

Succinate ^{1}H-MRS in a 4.7 Tesla animal-dedicated MRI device

Imaging was performed 37±11 days after the graft for the *Sdhb-/-* group versus 22±7 days for the WT group. Mice were placed in prone position under isoflurane anesthesia (4% for induction and 1.5% for maintenance in 1L/min air) with respiration monitoring.

^{1}H-MRS was performed in a dedicated small-animal 4.7 Tesla (T) MR system (Biospec 47/40 USR Bruker), using a ^{1}H quadrature transmit/receive body coil with a 3.5 cm inner diameter. An anatomical two-dimensional (2D) steady state free precession sequence (True FISP) was first acquired in two orthogonal planes. ^{1}H-MRS was then carried out using an optimized asymmetric Point REsolved SpectroScopy (PRESS) monovoxel acquisition (Fig. S1). Echo signals [Repetition Time (TR) = 3000 ms, Echo Time (TE) = 144 or 272 ms, Average = 512, with a volume of interest (VOI) size of 5×5×5 mm^3] were acquired during 25 min.

The MRS spectrum of succinic acid (HOOC-$(CH_2)_2$-COOH) presents a characteristic peak at 2.44 ppm, corresponding to the precession frequency of the CH_2 protons. The succinate peak was quantified by measuring the area under the peak using Topspin™ 2.0 software (Brüker corporation).

Patients

Patients were recruited from the French COMETE ('Cortico et Médullosurrénale: les Tumeurs Endocrines')-cohort of the Hypertension unit of the European Georges Pompidou Hospital (HEGP), Paris, France. Ethical approval for the study was obtained from the institutional review board [Comité de Protection des Personnes (CPP) Ile de France II] and written informed consent

to participate in the study was obtained from all patients. The procedures used for PPGL diagnosis and genetic testing were in accordance with international clinical practice guidelines (1). Mutation analysis of PPGL susceptibility genes was performed as previously described (28). When patients underwent surgery for PGL, fresh tumor samples were frozen immediately after surgical removal and stored in liquid nitrogen until processing following the COMETE collection procedures. Confirmation of diagnosis was performed by histology on paraffin-embedded formalin fixed samples.

Succinate detection by ^{1}H-MRS in patients at 3 Tesla

Combined MR images and MR spectroscopic scans of patients were acquired in a 3T MRI clinical scanner (Discovery MR750w GEMSOW, GE Medical Systems, Milwaukee, WI). ^{1}H-MRS spectra were acquired by PRESS based on the PROBE monovoxel sequence(29) and optimized for succinate and lactate detection, with TR: 2500 ms; TE: 144 ms; Nex: 512 (22 min acquisition) or 1024 (44 min acquisition). The Volume of Interest (VOI; 1.3 to 19 cm^3) was centered on the anatomical image to prevent lipid contamination from the tissue surrounding the tumor as previously described. (30)

MR images were acquired using a whole body (GEM Chest/Body/Pelvis;Body 24 AA3) or a head and neck (GEM Head/Neck/Chest; Head 24) phased-array multi-coil.

Detection of tumors and VOI positioning was performed on thin-section high-resolution T2-weighted fast spin-echo imaging in at least two orthogonal planes with the following

parameters: TR: 2500 ms; TE: 85 ms; echo train length: 19; slice thickness: 3 mm; spacing: 0.3; field of view: 14x14cm for neck or 42x42 cm for whole body coil; matrix: 320×320.

If necessary, an anatomical two-dimensional (2D) steady state free precession sequence (FIESTA CINE) was acquired with TR: 3.7 ms/TE: 1.4 ms; TI: 210ms; slice thickness: 5 mm; spacing: 1 mm; field of view: 14x14 cm for neck or 42x42 cm for whole body coil and/or a 3-dimensional angio-MR at arterial phase, after contrast agent administration of gadoterate meglumine 0.2 mL/kg with TR: 11.4 ms; TE: 2.2 ms; slice thickness: 0.8 mm; spacing: 0.4 mm; field of view: 30x27 cm.

A prescan algorithm was first acquired to adapt the transmitter and receiver gains and center frequency, the homogeneity of the magnetic field was optimized with the three-plane auto-shim procedure, and water suppression and automatic shimming of the single voxel were performed.

Measurement of succinate by gas chromatography-mass spectrometry.

Tumor samples from 15 mice (ten samples with *Sdhb* knockout and five WT controls) and from paragangliomas of four patients (patients #1, #5, #6 and #9) were processed by organic extraction with ethylacetate, derivatization with N,O-bis(trimethylsilyl) trifluoroacetamide with 1% trimethylchlorosilane, and analysed by gas chromatography-tandem mass spectrometry (GC-MS) on a GC-MS triple quadrupole (Scion TQ, Brüker Daltonics). Analytes were identified according to retention time and mass spectrum in selected reaction monitoring mode based on standard spectral reference libraries.

Immunohistochemistry

SDHA, SDHB, and SDHD protein expression were assessed on formalin-fixed paraffin embedded (FFPE) tumor samples by immunohistochemistry as previously described (16, 18, 22) using the following antibodies: anti-SDHA (ab14715, Abcam; 1:1000), anti-SDHB (HPA002868, Sigma-Aldrich Corp; 1:500) and anti-SDHD (HPA045727, Sigma-Aldrich Corp; 1:50).

SDH activity

SDH activity was investigated on frozen tumor samples using a spectrophotometrical assay, as previously described (31).

Results

In vivo detection of succinate in murine allografted tumors

The ^{1}H-MRS sequence was optimized *in vitro* (Fig. S1). In order to investigate whether *in vivo* detection of succinate could be assessed for the non-invasive identification of *SDH*-related tumors, a proof-of-concept pilot study was performed in a mouse model prior to patients' exploration. No animal model of SDH-related PPGL being available, we generated an allografted mouse model using immortalized mouse chromaffin cells (imCC) carrying a homozygous knockout of the *Sdhb* gene or their wild type (WT) counterparts (13). *Sdhb* knockout in tumors was confirmed by genotyping (Fig. 1A) and measurement of SDH enzymatic activity (Fig. 1B). Gas chromatography-tandem mass spectrometry (GC-MS) showed a massive accumulation of succinate in SDH-deficient tumors: 28.3 ± 9.5 nmol per mg protein in the *Sdhb*$^{-/-}$ group, versus 0.6 ± 0.7 nmol per mg protein in the control groups (Fig. 1C), confirming inhibition of SDH activity in *Sdhb*$^{-/-}$ tumors. ^{1}H-MRS was first tested in mice using a TE=272 ms and a fixed VOI size (125 mm^{3}) placed over the tumor mass of 13 *Sdhb*$^{-/-}$ and 16 WT allografted mice (Fig. 1D). The peak corresponding to lactate, indicative of anaerobic glycolysis was always present regardless of the tumor type. In contrast, the succinate peak was only detected in *Sdhb*$^{-/-}$ tumors, with a sensitivity and specificity of 100% (n= 13), in agreement with succinate accumulation caused by SDH inhibition (Fig. 1D and Fig. S2A). Measurements of succinate concentrations in *Sdhb*$^{-/-}$ tumor samples (n= 4) by GC-MS confirmed the MRS results. The succinate levels measured *in vitro* correlated with the area under the succinate peaks using an echo time (TE) of 272 ms (r^{2}=0.88; Fig. 1E). The results obtained in the 4.7 T magnet with TE=272 ms were repeated with TE=144 ms in 5 *Sdhb*$^{-/-}$ and 3 WT tumors, (Fig. 1F and Fig. S2B). At TE=144 ms, lactate was hardly

detectable while succinate was specifically observed in *Sdhb*$^{-/-}$ tumors. Again, GC-MS quantification of succinate performed in *Sdhb*$^{-/-}$ resected samples (n= 5) correlated with *in vivo* measures (r^2=0.70; Fig. 1G).

In vivo detection of succinate in patients

Nine patients presenting with PCC, cervical, and/or abdominal PGLs were recruited at the Hypertension unit of the European Georges Pompidou Hospital (Table 1). All patients benefited from genetic counseling in accordance with the Endocrine Society clinical practice guidelines (1). Before undergoing SUCCES with ^{1}H-MRS, a germline *SDHx* gene mutation was identified in four patients (one *SDHB*, one *SDHC,* and two *SDHD*), while no mutation was identified for the other five patients.

Genetic testing identified a variant of unknown significance (VUS) in the *SDHB* gene of Patient #1 (c.740T>G=p.Met247Arg), a 33-year-old male with two PGLs and a predominant noradrenergic secretion profile. In the cervical PGL of this patient, the ^{1}H-MRS signal of succinate was unequivocally discernable at 2.44 ppm using 1024 averages and a 4.6 cm^3 VOI size (Fig. 2A). Sensitivity and specificity were explored by reducing the scan repeats from 1024 to 512 averages and the VOI size from 4.6 to 1.5 cm^3: the succinate peak was still clearly detected in low sensitivity conditions in the cervical PGL (Fig. 2A), as well as in the abdominal tumor mass (Fig. 2B), but not in the liver, showing the persistence of SDH activity in this healthy organ, expected to be heterozygous for the mutation (Fig. 2C). The pathogenicity of this newly-described variant suggested by ^{1}H-MRS was supported by the loss of heterozygozity (LOH) at

the *SDHB* locus in DNA extracted from the resected abdominal PGL (Fig. 2D) and confirmed by three functional tests: SDHB-negative (unspecific weak diffuse signal) and SDHD-positive immunohistochemistries (Fig. 2E), loss of SDH enzymatic activity (Fig. 2F), and succinate accumulation measured by GC-MS (Fig. 2G).

The succinate peak was observed in the tumors of the three other *SDHx* patients using scan repeats of 1024 and 512 averages (Fig. S3). Interestingly, a choline peak at 3.2 ppm was associated with the succinate peak in each of the *SDHx*-mutated tumors. In contrast, neither succinate nor choline peaks were observed in tumors from patients without *SDHx* mutations (Fig. 3 and Fig. S4). In Patient #5, immunohistochemistry of tumor samples showed SDHB and SDHA-positive, and SDHD-negative staining, while GC-MS analysis confirmed the absence of succinate accumulation (Fig. 3B and C).

Unexpected SDHA mutation identified by SUCCES

Surprisingly, a small but significant peak above baseline was detected in an abdominal PGL from a patient with an apparently sporadic form of the disease (Fig. 4A.) This patient was a 48-year-old man suffering from a single abdominal PGL with no family history of PPGL. Following comprehensive genetic counseling according to the international guidelines, the search for mutations of *SDHB, SDHC,* and *SDHD* genes returned negative. Nevertheless, the presence of a succinate peak in the tumor of this patient prompted us to sequence the *SDHA* gene of this patient, which identified a c.91C>T=p.Arg31Ter mutation (Fig. 4B), previously reported in Dutch patients with PPGL(16) or GIST (32). After the patient had undergone surgery, additional

analyses of his tumor showed negative SDHA and SDHB, and positive SDHD immunohistochemistry (Fig. 4C). GC-MS confirmed the accumulation of succinate (Table 1), and validated the rare and unexpected *SDHA*-mutated status of this patient that had been initially stratified as a sporadic case.

Discussion

Here, we report the non-invasive detection of succinate by *in vivo* Magnetic Resonance Spectroscopy in tumors of PPGL patients carrying *SDHx* genes mutations, but not in those of patients without *SDHx* mutations. Interestingly, in an *Sdhb-/-* mouse tumor model this succinate peak is correlated with the concentrations of succinate measured in the resected tumors by GC-MS.

Demonstration of SDH inactivation is currently based on *in vitro* analyses of tissue samples: immunohistochemical analyses of SDHB, SDHA, and SDHD expression in FFPE tissues (16, 18, 22), direct succinate measurements on frozen tumor samples by nuclear magnetic resonance (NMR) spectroscopy (15, 19, 20, 23), GC-MS, or liquid chromatography mass spectroscopy (LC-MS) (13, 17, 21). Recently, Varoquaux et al reported *in vivo* detection of succinate using ^{1}H-MRS in 6 patients with head and neck PGL (3 *SDHD*, 1 *SDHB* and 2 sporadic cases). Although the spectra quality was considered as low in the 2 sporadic cases, and uninterpretable in one *SDHD*-mutated tumor, a succinate peak was also only detected in three *SDHx*-mutated tumors (33). In the present study, we show that ^{1}H-MRS also detects succinate in abdominal PGL and in genes encoding all four SDH subunits. Moreover, we performed longer acquisition time (512 and 1024 averages, versus 120 in the Varoquaux et al study), which allowed an immediate interpretation of spectra, without the need of post-processing the data.

The benefits of assessing this tumor hallmark in patients with *SDHx*-related tumors are important in several aspects. SUCCES would allow stratifying these patients or classifying VUS as deleterious mutations with no need of tissue sampling. Patient #9 carried a single abdominal PGL diagnosed at age 48, without a family history for this disease. According to international

guidelines, *SDHB, SDHC,* and *SDHD* genetic testing were performed in this patient, but not *SDHA,* which would have been prescribed only after surgery, in case of SDHA negative IHC (1). In such a case, exploring the patient with ^{1}H-MRS and detecting the succinate peak orientated us without hesitation towards *SDHA* sequencing, leading to early identification of the mutation. SDHA immunohistochemistry is not is not included in international guidelines and is not a standard procedure, thus it is likely that this mutation would have been missed in most instances. In Patient #1, an *SDHB* gene VUS was identified, while SDHB IHC showed a potentially misleading, weak diffuse signal, previously reported in some PPGL with *SDHx* genes mutations (18). Hence, in this other case, the ^{1}H-MRS succinate peak was particularly informative to validate the functionality of the *SDHB* mutation.

SDHx-mutation carriers are at risk of developing multiple PGLs, and *SDHB*-mutated carriers are predisposed to metastatic forms of the disease. Knowledge of the *SDHx*-mutated status is critical for the follow-up and clinical management of these patients and of their relatives. Based on an early knowledge of the *SDHx* mutational status, surgeons may decide to adapt their procedures, especially for *SDHB* cases. For non-operable tumors, therapeutic choices may also take advantage from this information. For example, studies have suggested that *SDHB*-mutation carriers may be better responders to high doses of ^{131}I-MIBG (34), sunitinib (35) or temozolomide treatments (36). Although these results will need to be evaluated in larger, prospective and comparative studies, they nevertheless pave the way towards personalized medicine for inherited PPGL.

Overall, the clinical value of SUCCES lies in its capacity to assess for the presence of succinate repeatedly over the time course of the disease, for clinical surveillance, post-operative follow-

up, and evaluation of treatment efficacy (17). *In vivo* estimation of succinate could help classifying a dubious lesion detected during surveillance and to demonstrate the causality of SDH deficiency in tumors identified in *SDHx*-mutated patients. This would be particularly helpful in cases for which surgery is not necessary, such as prolactin-secreting pituitary adenomas recently described in *SDHx* mutation carriers (37). Because of the small size of these tumors, the feasibility of SUCCESS may however be more difficult in these cases.

Animal experiments demonstrated that the area under the succinate peak of the ^{1}H-MRS spectra is correlated with the concentrations of succinate measured in the resected tumors by GC-MS. Future studies in larger groups will be needed to show if this correlation holds also in patients. If this turned out to be the case and given that succinate concentrations in tumors reflect the metabolic activity of SDH-deficient tumor cells, then SUCCES would produce a quantifiable surrogate marker of radiation and/or chemotherapy efficacy for the patients.

Interestingly, other metabolites have been shown *in vitro* to discriminate between different types of inherited PPGL (20). In future studies, it may also be addressed whether these metabolites can also be observed 1H-MRS and used as supplemental tools. For example, Imperiale et al recently reported in a case of sporadic pheochromocytoma that catecholamines are indeed detectable by ^{1}H-MRS (38).

The present proof-of-concept study has shown that SUCCES is highly sensitive, reliable, and specific for the detection of the *SDHx* mutations that lead to inhibition of SDH activity. The next step in order to fully define the place of this new method in the clinical management of PPGL is to test the method in larger series of patients and define the best conditions for routine clinical applications. In that respect, we occasionally observed, in both groups of patients, a blunt

signal centered at 1.2 ppm. This signal corresponds to adipose tissue surrounding the tumor that is not always straightforward to avoid even with strict intra-tumor positioning of the VOI in which ^{1}H-MRS is performed. Since MRS data are usually displayed with a *y* scale normalized on the highest peak of the spectrum, the presence of a significant lipid signal may modify the threshold for succinate detection in small lesions. Averaging more spectra increases the signal-to-noise ratio but also increases scan duration, which may not be applicable to all patients. For abdominal tumors, respiratory gating should be considered to reduce the lipid peak and improve the quality of spectra, as previously reported for in vivo catecholamine detection (38). Using 512 scan averages appears to be sufficient for reliable succinate detection in tumors with *SDHx* genes mutation. However, this may limit the quality of spectra for small or highly necrotic tumors, as shown in the case of patient #3 (Fig. S3B), for whom successful interpretation could only be achieved after 1024 scan averages. Therefore the minimal tumor size for reliable measurements of succinate needs to be addressed in future prospective studies. Fortunately, this ^{1}H-MRS sequence is easy to implement in any clinical MRI scanner using standard hardware and software already in place in many imaging departments.

Finally, it is noteworthy that the succinate peak was always associated in human PPGL with a peak resonating at 3.2 ppm on the ^{1}H-MRS spectra, most probably corresponding to choline. Such a peak was only seen in tumors from the patients carrying *SDHx* mutations. Previous *in vitro* NMR studies never reported such a choline increase in SDH-related tumors. However, a similar peak is also observed in the spectra of both SDH-mutated PGL evaluated by *in vivo* 1H-MRS in the Varoquaux et al study (33). The accuracy of this observation will need to be further validated both *in vivo* and *in vitro*, in SDH as well as in other oncogenic mutations of metabolic

pathways. It is worth noting that choline is a methyl donor in the S-adenosylmethionine pathway involved in DNA and histone methylation. Hence, if confirmed, the choline peak that we observed here may be related to the disrupted methylation phenotype recently identified in SDH-deficient tumors (13).

In conclusion, we present here a robust and simple method that can be used routinely to demonstrate the presence of succinate in the tumors of PPGL patients. Considering its excellent sensitivity, specificity, and innocuousness, SUCCES deserves to be tested in large multicentric series in order to define its place in the clinical guidelines of PPGL management as well as in other SDH-related tumors such as GIST and renal clear cell carcinomas.

Acknowledgments

We are grateful to Prof. Pierre-François Plouin and Dr Guillaume Bobrie for their clinical contribution to the study, and to Prof. Catherine Oppenheim and Stephanie Lion for sharing their expertise. We thank Daniel Balvay for helpful discussions, Brigitte Lambert (Radiology, HEGP) and Marion Uettwiller (General Electrics Healthcare) for technical assistance, and Catherine Tritscher for administrative assistance. We thank the technical staff of the Genetic department of HEGP (especially Françoise Le Quellec, Caroline Travers, Nirubiah Thurairajasingam) led by Prof. Xavier Jeunemaitre, Jean-Michaël Mazzella, and Samir Jocelyn Do Rego for their contribution to the study. We thank Daniel Tennant for helpful discussion. C. Lepoutre-Lussey is funded by the CARPEM project. A. Bellucci received a fellowship from

Fondation pour la Recherche Médicale. A. Buffet received a fellowship from the ITMO Cancer - Plan Cancer 2014-2019.

References

1. Lenders JW, Duh QY, Eisenhofer G, Gimenez-Roqueplo AP, Grebe SK, Murad MH, et al. Pheochromocytoma and paraganglioma: an endocrine society clinical practice guideline. J Clin Endocrinol Metab. 2014;99:1915-42.
2. Favier J, Amar L, Gimenez-Roqueplo AP. Paraganglioma and phaeochromocytoma: from genetics to personalized medicine. Nat Rev Endocrinol. 2015;11:101-11.
3. Janeway KA, Kim SY, Lodish M, Nose V, Rustin P, Gaal J, et al. Defects in succinate dehydrogenase in gastrointestinal stromal tumors lacking KIT and PDGFRA mutations. Proceedings of the National Academy of Sciences of the United States of America. 2011;108:314-8.
4. Vanharanta S, Buchta M, McWhinney SR, Virta SK, Peczkowska M, Morrison CD, et al. Early-onset renal cell carcinoma as a novel extraparaganglial component of SDHB-associated heritable paraganglioma. Am J Hum Genet. 2004;74:153-9.
5. Baysal BE, Ferrell RE, Willett-Brozick JE, Lawrence EC, Myssiorek D, Bosch A, et al. Mutations in SDHD, a mitochondrial complex II gene, in hereditary paraganglioma. Science. 2000;287:848-51.
6. Warburg O. Ueber den stoffwechsel der tumoren. Constable, London. 1930.
7. Tomlinson IP, Alam NA, Rowan AJ, Barclay E, Jaeger EE, Kelsell D, et al. Germline mutations in FH predispose to dominantly inherited uterine fibroids, skin leiomyomata and papillary renal cell cancer. Nat Genet. 2002;30:406-10.
8. Yan H, Parsons DW, Jin G, McLendon R, Rasheed BA, Yuan W, et al. IDH1 and IDH2 mutations in gliomas. The New England journal of medicine. 2009;360:765-73.
9. Morin A, Letouze E, Gimenez-Roqueplo AP, Favier J. Oncometabolites-driven tumorigenesis: From genetics to targeted therapy. Int J Cancer. 2014;135:2237-48.
10. Gimenez-Roqueplo AP, Caumont-Prim A, Houzard C, Hignette C, Hernigou A, Halimi P, et al. Imaging work-up for screening of paraganglioma and pheochromocytoma in SDHx mutation carriers: a multicenter prospective study from the PGL.EVA Investigators. The Journal of clinical endocrinology and metabolism. 2013;98:E162-73.
11. Amar L, Baudin E, Burnichon N, Peyrard S, Silvera S, Bertherat J, et al. Succinate dehydrogenase B gene mutations predict survival in patients with malignant pheochromocytomas or paragangliomas. The Journal of clinical endocrinology and metabolism. 2007;92:3822-8.
12. Gimenez-Roqueplo AP, Favier J, Rustin P, Rieubland C, Crespin M, Nau V, et al. Mutations in the SDHB gene are associated with extra-adrenal and/or malignant phaeochromocytomas. Cancer Res. 2003;63:5615-21.
13. Letouze E, Martinelli C, Loriot C, Burnichon N, Abermil N, Ottolenghi C, et al. SDH mutations establish a hypermethylator phenotype in paraganglioma. Cancer Cell. 2013;23:739-52.
14. Selak MA, Armour SM, MacKenzie ED, Boulahbel H, Watson DG, Mansfield KD, et al. Succinate links TCA cycle dysfunction to oncogenesis by inhibiting HIF-alpha prolyl hydroxylase. Cancer Cell. 2005;7:77-85.

15. Imperiale A, Moussallieh FM, Roche P, Battini S, Cicek AE, Sebag F, et al. Metabolome profiling by HRMAS NMR spectroscopy of pheochromocytomas and paragangliomas detects SDH deficiency: clinical and pathophysiological implications. Neoplasia. 2015;17:55-65.
16. Korpershoek E, Favier J, Gaal J, Burnichon N, van Gessel B, Oudijk L, et al. SDHA immunohistochemistry detects germline SDHA gene mutations in apparently sporadic paragangliomas and pheochromocytomas. The Journal of clinical endocrinology and metabolism. 2011;96:E1472-6.
17. Lendvai N, Pawlosky R, Bullova P, Eisenhofer G, Patocs A, Veech RL, et al. Succinate-to-fumarate ratio as a new metabolic marker to detect the presence of SDHB/D-related paraganglioma: initial experimental and ex vivo findings. Endocrinology. 2014;155:27-32.
18. Menara M, Oudijk L, Badoual C, Bertherat J, Lepoutre-Lussey C, Amar L, et al. SDHD immunohistochemistry: a new tool to validate SDHx mutations in pheochromocytoma/paraganglioma. J Clin Endocrinol Metab. 2015;100:E287-91.
19. Rao JU, Engelke UF, Rodenburg RJ, Wevers RA, Pacak K, Eisenhofer G, et al. Genotype-specific abnormalities in mitochondrial function associate with distinct profiles of energy metabolism and catecholamine content in pheochromocytoma and paraganglioma. Clin Cancer Res. 2013;19:3787-95.
20. Rao JU, Engelke UF, Sweep FC, Pacak K, Kusters B, Goudswaard AG, et al. Genotype-specific differences in the tumor metabolite profile of pheochromocytoma and paraganglioma using untargeted and targeted metabolomics. J Clin Endocrinol Metab. 2015;100:E214-22.
21. Richter S, Peitzsch M, Rapizzi E, Lenders JW, Qin N, de Cubas AA, et al. Krebs cycle metabolite profiling for identification and stratification of pheochromocytomas/paragangliomas due to succinate dehydrogenase deficiency. J Clin Endocrinol Metab. 2014;99:3903-11.
22. van Nederveen FH, Gaal J, Favier J, Korpershoek E, Oldenburg RA, de Bruyn EM, et al. An immunohistochemical procedure to detect patients with paraganglioma and phaeochromocytoma with germline SDHB, SDHC, or SDHD gene mutations: a retrospective and prospective analysis. Lancet Oncol. 2009;10:764-71.
23. Pollard PJ, Briere JJ, Alam NA, Barwell J, Barclay E, Wortham NC, et al. Accumulation of Krebs cycle intermediates and over-expression of HIF1alpha in tumours which result from germline FH and SDH mutations. Human molecular genetics. 2005;14:2231-9.
24. Andronesi OC, Kim GS, Gerstner E, Batchelor T, Tzika AA, Fantin VR, et al. Detection of 2-hydroxyglutarate in IDH-mutated glioma patients by in vivo spectral-editing and 2D correlation magnetic resonance spectroscopy. Sci Transl Med. 2012;4:116ra4.
25. Choi C, Ganji SK, DeBerardinis RJ, Hatanpaa KJ, Rakheja D, Kovacs Z, et al. 2-hydroxyglutarate detection by magnetic resonance spectroscopy in IDH-mutated patients with gliomas. Nat Med. 2012;18:624-9.
26. Elkhaled A, Jalbert LE, Phillips JJ, Yoshihara HA, Parvataneni R, Srinivasan R, et al. Magnetic resonance of 2-hydroxyglutarate in IDH1-mutated low-grade gliomas. Science translational medicine. 2012;4:116ra5.
27. Harada K, Honmou O, Liu H, Bando M, Houkin K, Kocsis JD. Magnetic resonance lactate and lipid signals in rat brain after middle cerebral artery occlusion model. Brain Res. 2007;1134:206-13.

28. Burnichon N, Vescovo L, Amar L, Libe R, de Reynies A, Venisse A, et al. Integrative genomic analysis reveals somatic mutations in pheochromocytoma and paraganglioma. Human molecular genetics. 2011;20:3974-85.
29. Webb PG, Sailasuta N, Kohler SJ, Raidy T, Moats RA, Hurd RE. Automated single-voxel proton MRS: technical development and multisite verification. Magn Reson Med. 1994;31:365-73.
30. Agarwal M, Chawla S, Husain N, Jaggi RS, Husain M, Gupta RK. Higher succinate than acetate levels differentiate cerebral degenerating cysticerci from anaerobic abscesses on in-vivo proton MR spectroscopy. Neuroradiology. 2004;46:211-5.
31. Rustin P, Chretien D, Bourgeron T, Gerard B, Rotig A, Saudubray JM, et al. Biochemical and molecular investigations in respiratory chain deficiencies. Clin Chim Acta. 1994;228:35-51.
32. Oudijk L, Gaal J, Korpershoek E, van Nederveen FH, Kelly L, Schiavon G, et al. SDHA mutations in adult and pediatric wild-type gastrointestinal stromal tumors. Mod Pathol. 2013;26:456-63.
33. Varoquaux A, le Fur Y, Imperiale A, Reyre A, Montava M, Fakhry N, et al. Magnetic resonance spectroscopy of paragangliomas: new insights into in vivo metabolomics. Endocr Relat Cancer. 2015;22:M1-8.
34. Gonias S, Goldsby R, Matthay KK, Hawkins R, Price D, Huberty J, et al. Phase II study of high-dose [131I]metaiodobenzylguanidine therapy for patients with metastatic pheochromocytoma and paraganglioma. J Clin Oncol. 2009;27:4162-8.
35. Jimenez C, Rohren E, Habra MA, Rich T, Jimenez P, Ayala-Ramirez M, et al. Current and future treatments for malignant pheochromocytoma and sympathetic paraganglioma. Current oncology reports. 2013;15:356-71.
36. Hadoux J, Favier J, Scoazec JY, Leboulleux S, Al Ghuzlan A, Caramella C, et al. SDHB mutations are associated with response to temozolomide in patients with metastatic pheochromocytoma or paraganglioma. Int J Cancer. 2014;135:2711-20.
37. Xekouki P, Szarek E, Bullova P, Giubellino A, Quezado M, Mastroyannis SA, et al. Pituitary adenoma with paraganglioma/pheochromocytoma (3PAs) and succinate dehydrogenase defects in human and mice. The Journal of clinical endocrinology and metabolism. 2015:jc20144297.
38. Imperiale A, Battini S, Averous G, Mutter D, Goichot B, Bachellier P, et al. In vivo detection of catecholamines by magnetic resonance spectroscopy: A potential specific biomarker for the diagnosis of pheochromocytoma. Surgery. 2015. Epub May 1

Table 1: Characteristics of the 9 patients and 10 tumors analyzed by ^{1}H-MRS at 3 Tesla

Patient	Gender	Age	Gene	Mutation type	Multiple locations	Type of tumor analyzed	Largest tumor diameter (mm)	VOI size (cm^3)	Succinate level on GC-MS (nmol/mg protein)
1	M	33	*SDHB*	c.740T>G p.Met247Arg	Yes	VPGL	80	4.6 α 1.5	ND
						APGL	94	19.2	89.3
2	M	70	*SDHC*	c.397C>T p.Arg133Ter	No	VPGL	42	3.7	ND
3	F	32	*SDHD*	c.210G>T p.Arg70Ser	Yes	CBPGL	24	1.5	ND
4	M	41	*SDHD*	c.325C>T p.Gln109Ter	Yes	CBPGL	39	3.6	ND
5	M	25	none	NA	No	PCC	55	6.2	0.84
6	M	60	none	NA	No	APGL	35	4.2	0.54
7	F	74	none	NA	Yes	CBPGL	30	1.3	ND
8	M	47	none	NA	No	PCC	30	5.8	ND
9	M	48	*SDHA*	c.91C>T p.Arg31Ter	No	APGL	50	12	72.17

1-H-MRS: proton magnetic resonance spectroscopy; PCC: pheochromocytoma, APGL: abdominal paraganglioma ; CBPGL: carotid body paraganglioma; VPGL: carotid body paraganglioma; VOI: Volume of Interest; NA: non applicable; ND: Not determined.

Figure Legends

Fig. 1. **SUCCES in *Sdhb*$^{-/-}$ allografted tumors in mice. (A)** Genotyping of *Sdhb* gene locus in DNA extracted from tumors derived from *Sdhb*$^{-/-}$ and WT (*Sdhb*$^{lox/lox}$) cells allografted in mice. The deletion of exon 2 (Δex2, 460 bp) is visible in tumors from *Sdhb*$^{-/-}$ grafted cells while the floxed allele (900 pb) is shown in the *Sdhb*$^{lox/lox}$ grafted mice. In both tumor types, a WT DNA band (845 bp) originating from the supporting cells of the allografted mice (fibroblasts, endothelial cells) is visible. **(B)** *Sdhb*$^{-/-}$ derived tumors display an unequivocal decrease in SDH activity measured by spectrophotometry. **(C)** Massive accumulation of succinate measured by gas chromatography-tandem mass spectrometry (GC-MS) in *Sdhb*$^{-/-}$ derived tumors, which is not seen in *Sdhb*$^{lox/lox}$-derived tumors. **(D)** ^{1}H-MRS spectra of tumor masses in mice allografted with WT (green spectra) or *Sdhb*$^{-/-}$ (blue spectra) cells using a TE=272 ms. The lactate peak was present regardless of the tumor type while the succinate peak was only detected in *Sdhb*$^{-/-}$ tumors. **(E)** Succinate levels measured *in vitro* by GC-MS correlate with the area under the succinate peaks (AUP) at TE=272 ms. **(F)** and **(G)** show the same data as in A and B respectively, but at TE= 144 ms.

Fig. 2: SUCCES in a patient with an *SDHB* gene mutation. (A) ^{1}H-MRS spectra of the right cervical PGL of Patient #1. A succinate peak was detected in the cervical PGL with two different averages (1024 and 512) and two different VOI sizes (4.6 and 1.5 cm3). **(B)** Applying the PRESS sequence to the abdominal tumor mass of the same patient permits to detect a succinate peak. **(C)** In the healthy liver, the absence of a peak demonstrates the specificity of the method. **(D)**

Genetic testing identified a variant of unknown significance in the *SDHB* gene with a loss of heterozygozity in tumor DNA extracted from the resected abdominal PGL. **(E)** SDHB immunochemistry (IHC) leads to an unspecific weak diffuse signal in tumor cells while endothelial cells (arrows) are strongly labeled (upper part). A positive staining is shown after SDHD IHC (lower part). Scale bar = 50 µm. **(F)** Significant reduction of SDH activity in Patient #1 (blue line) as compared to **(G)** Patient #6, a case without *SDHx* mutation.

Fig. 3: SUCCES in a patient without *SDHx* gene mutation. (A) Absence of a succinate peak in the ^{1}H-MRS spectrum of Patient #5's PCC with 1024 averages. **(B)** Unequivocal positive granular staining after SDHB and SDHA IHC (left), and negativity of SDHD IHC (right). Scale bar = 50 µm. **(C)** Low level of succinate in the tumor measured by GC-MS.

Fig. 4: SUCCES in a patient with a *SDHA* gene mutation. (A) ^{1}H-MRS spectra in Patient #9's abdominal PGL. A small succinate peak was detected with 512 averages and a 12 cm^{3} VOI size. **(B)** Results of genetic testing that identified a c. 91C>T variant in the *SDHA* gene. **(C)** SDHA and SDHB immunochemistry (IHC) lead to unspecific weak diffuse signals in tumor cells while endothelial cells are strongly labeled. In contrast, SDHD IHC shows a positive staining. Scale bars = 50 µm.

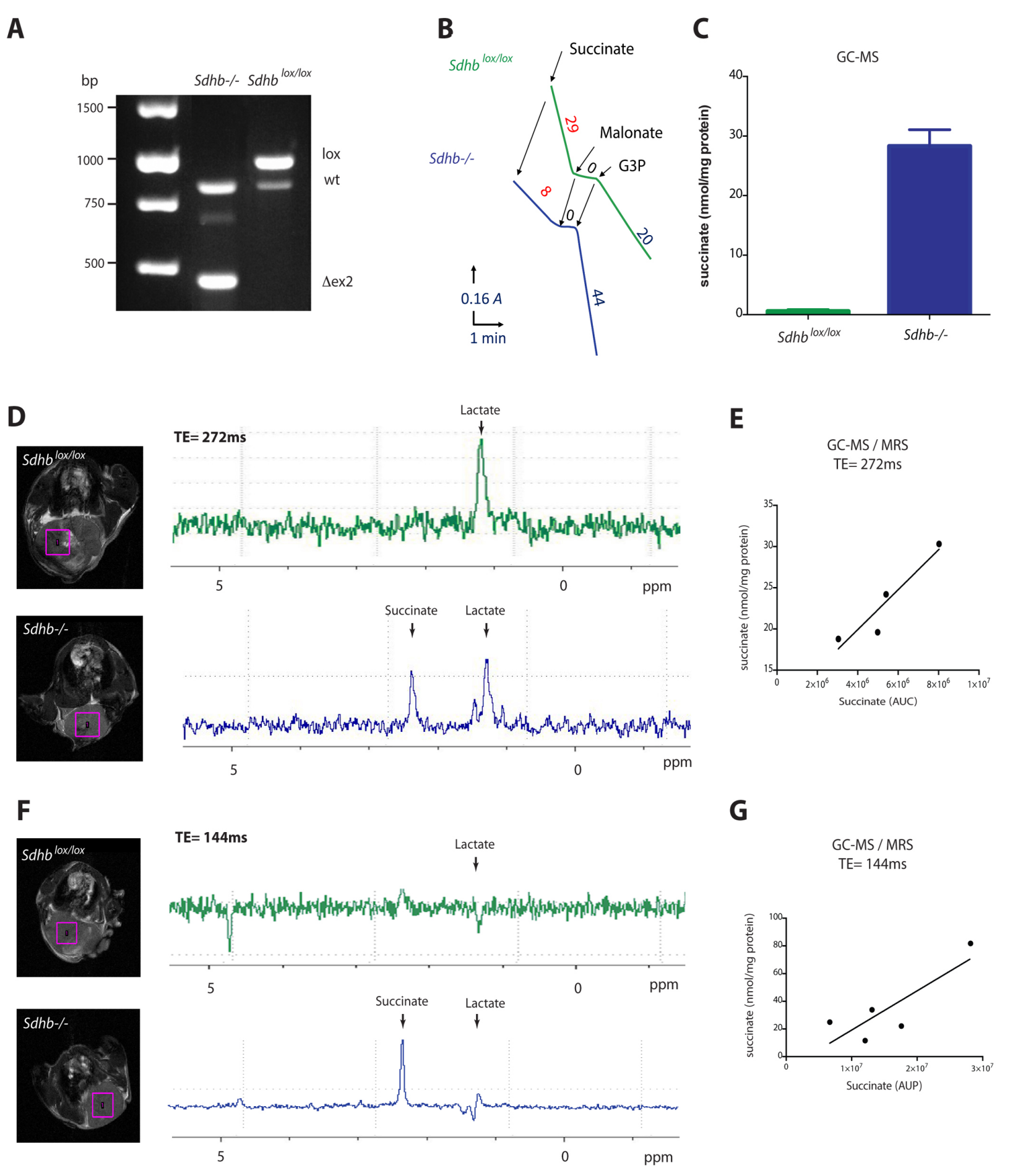
A
bp
Sdhb-/-
Sdhb lox/lox
1500
1000
750
500
lox
wt
Δex2
B
Sdhb lox/lox
Succinate
29
Malonate
Sdhb-/-
0
G3P
8
0
20
44
0.16 A
1 min
C
GC-MS
succinate (nmol/mg protein)
40
30
20
10
0
Sdhb lox/lox
Sdhb-/-
D
Sdhb lox/lox
Sdhb-/-
TE= 272ms
Lactate
5
0
ppm
Succinate
Lactate
5
0
ppm
E
GC-MS / MRS
TE= 272ms
succinate (nmol/mg protein)
35
30
25
20
15
0
2x10^6
4x10^6
6x10^6
8x10^6
1x10^7
Succinate (AUC)
F
Sdhb lox/lox
Sdhb-/-
TE= 144ms
Lactate
5
0
ppm
Succinate
Lactate
5
0
ppm
G
GC-MS / MRS
TE= 144ms
succinate (nmol/mg protein)
100
80
60
40
20
0
1x10^7
2x10^7
3x10^7
Succinate (AUP)

FIGURE 1

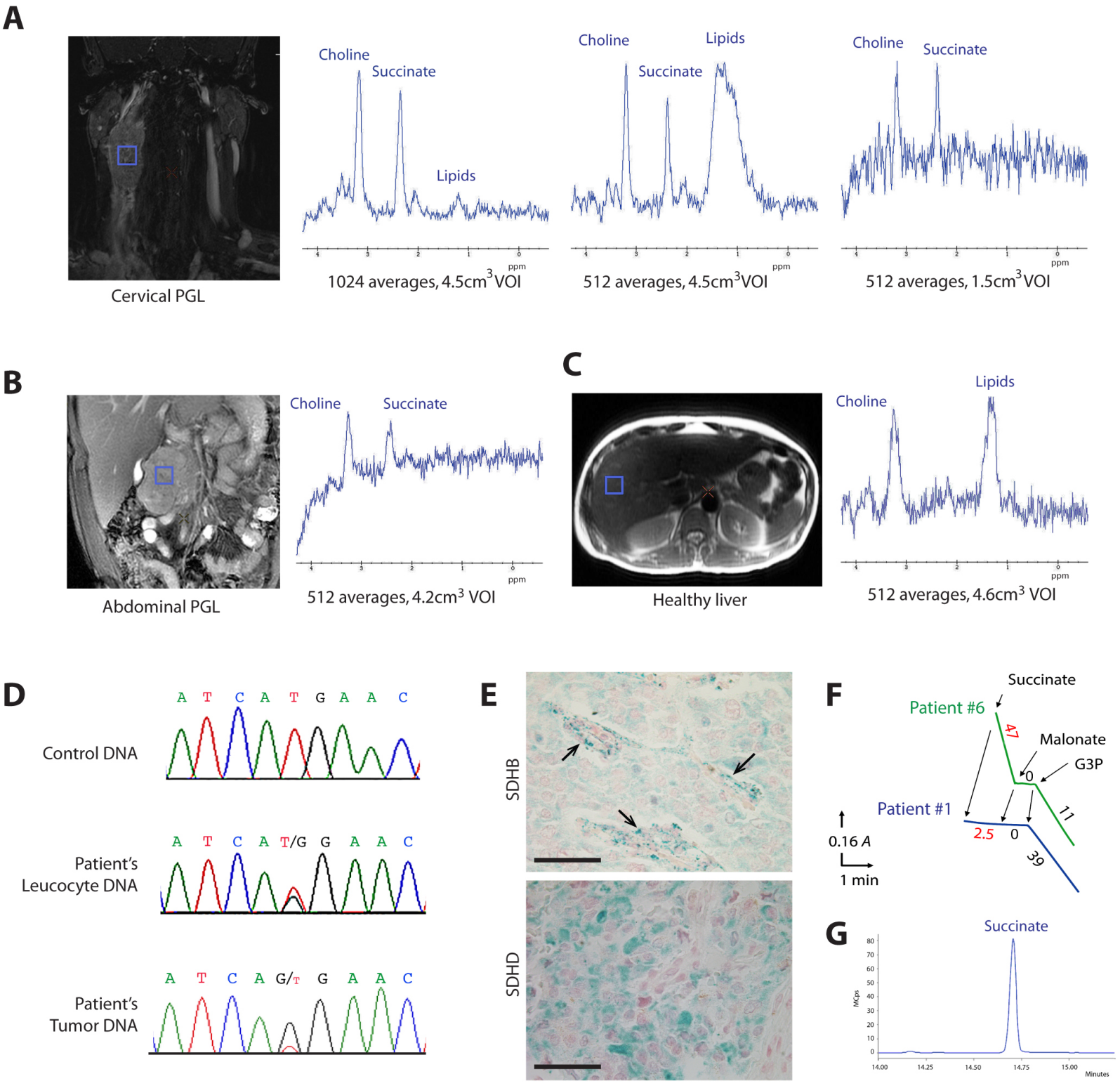
A
Choline
Succinate
Lipids
ppm
Cervical PGL
1024 averages, 4.5cm3 VOI
Choline
Lipids
Succinate
512 averages, 4.5cm3 VOI
Choline
Succinate
512 averages, 1.5cm3 VOI
B
Choline
Succinate
Abdominal PGL
512 averages, 4.2cm3 VOI
C
Lipids
Choline
Healthy liver
512 averages, 4.6cm3 VOI
D
A T C A T G A A C
Control DNA
A T C A T/G G A A C
Patient's Leucocyte DNA
A T C A G/T G A A C
Patient's Tumor DNA
E
SDHB
SDHD
F
Succinate
Patient #6
47
Malonate
G3P
0
11
Patient #1
2.5
0
39
0.16 A
1 min
G
Succinate
MCps
Minutes

FIGURE 2

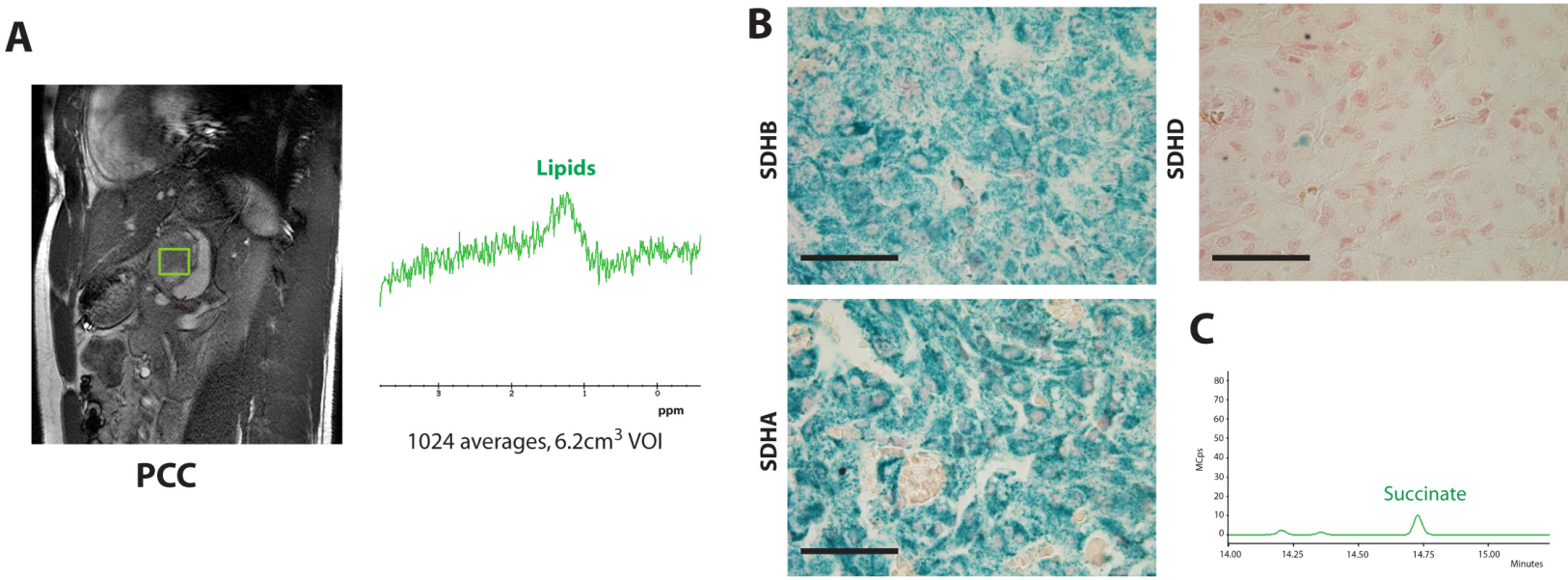
A
PCC
Lipids
5
2
1
0
ppm
1024 averages, 6.2cm3 VOI
B
SDHB
SDHD
SDHA
C
80
70
60
50
40
30
20
10
0
MCps
Succinate
14.00
14.25
14.50
14.75
15.00
Minutes

FIGURE 3

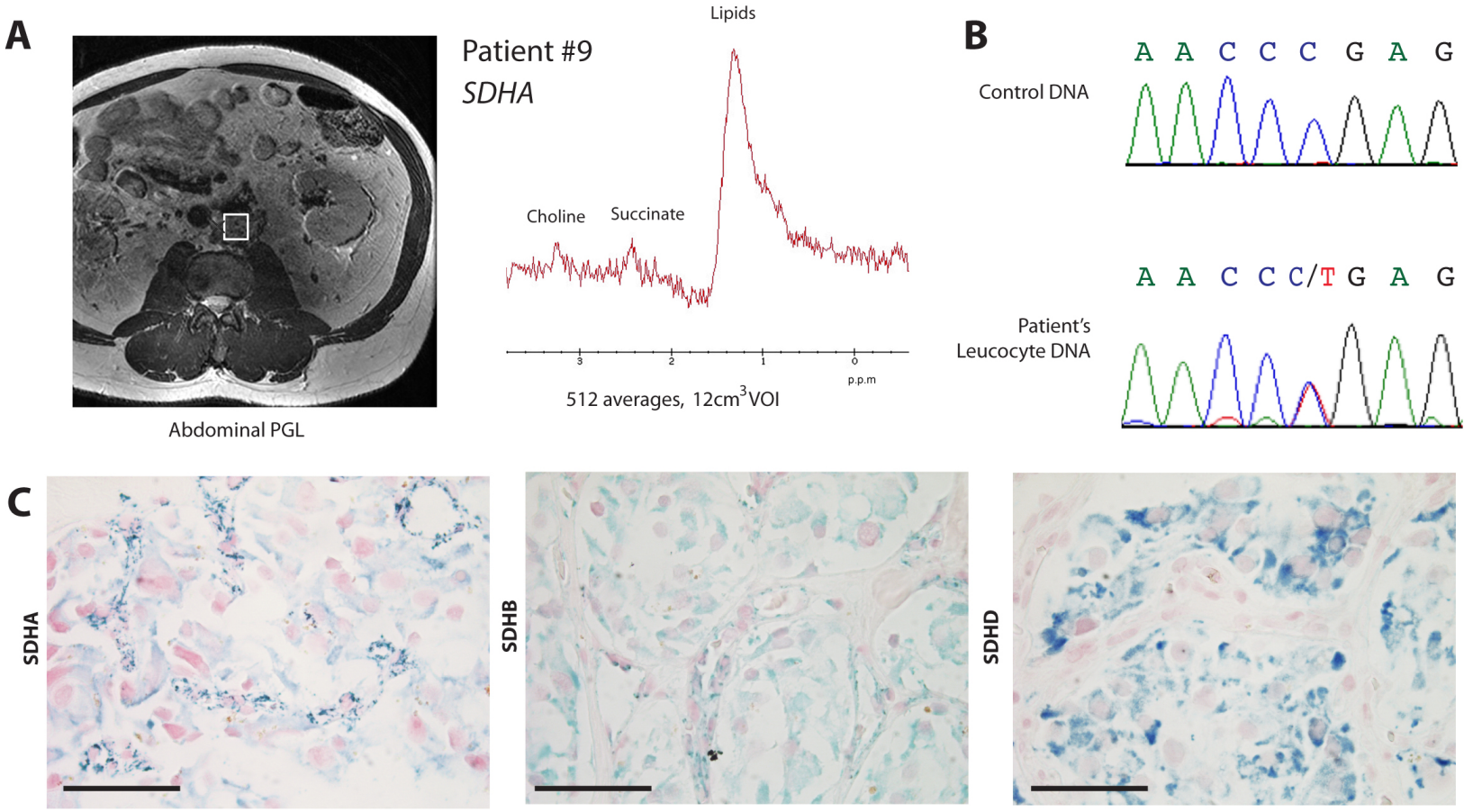
A
Abdominal PGL
Patient #9
SDHA
Lipids
Choline
Succinate
3
2
1
0
p.p.m
512 averages, 12cm3VOI
B
Control DNA
A A C C C G A G
Patient's
Leucocyte DNA
A A C C C/T G A G
C
SDHA
SDHB
SDHD

FIGURE 4